PHYSICAL REVIEW B VOLUME 9, NUMBER 10 15 MAY 1974

Lattice dynamics of aluminum: An investigation of exchange and correlation effects

J. Hafner*
Institut für Theoretische Physik, Technische Hochschule Wien, Austria

P. Schmuck†
Institut für Neutronenphysik und Reaktortechnik, Kernforschungszentrum Karlsruhe, Germany

(Received 21 December 1973)

Using Harrison's first-principles, nonlocal pseudopotential theory, an investigation was made to determine the influence of the electronic exchange and correlation interactions on the lattice dynamics and on the structural, cohesive, and electronic properties of aluminum. Different varieties of the local statistical $X\alpha$ exchange and correlation approximation are used to describe the core-core and conduction-band–core interactions. Exchange and correlation among the conduction electrons are taken into account by using different modified forms of the dielectric function. It is shown that a correct formulation of the conduction-band–core interaction is crucial for a correct description of atomic as well as electronic properties. The Lindgren approximation to this potential allows a nearly perfect reproduction of the experimental dispersion relations, but is shown to be inappropriate for the calculation of structural, cohesive, and electronic properties. The conventional $\rho_{\text{core}}^{1/3}$ ansatz for this potential, while being only moderately successful in the phonon calculations, still yields the best over-all picture of the properties of metallic aluminum. The remaining discrepancies between theory and experiment are to be attributed to the too long range of the $\rho^{1/3}$ exchange and correlation potential. Conduction-electron exchange and correlation are of only minor importance in the calculation of static crystal properties. In the lattice-dynamical calculations, the exchange and correlation corrections to the Hartree dielectric function strongly reduce the phonon frequencies. Different forms proposed for this correction are analyzed. It is demonstrated that the long-wavelength limit of the correction function most effectively influences the phonon energies. The satisfaction of the compressibility sum rule is a neccesary, but not sufficient condition for a correct description of the dispersion relations.

I. INTRODUCTION

The use of the pseudopotential or model-potential approach to the electron-ion interaction in determining the lattice dynamics of simple metals has become widespread since its introduction by Toya[1] and Cochran.[2] The problem can be considered from two different points of view. Formally, dispersion relations may be computed from a suitably chosen model potential whose parameters are determined to reproduce the experimental results from neutron spectroscopy.[3] On the other hand, one can try to derive the pseudopotential from first principles[4] and then use this potential to construct the phonon-dispersion curves. A number of rather successful calculations of the former kind have been presented for Al.[3,5–14] No unequivocal conclusion on the appropriateness of the different model potentials and screening functions being used arises from this computations, and the application of these potentials to the calculation of other crystal properties (such as the binding energy, the structural stability, the equilibrium lattice spacing, etc.), is only fairly successful. A first-principles calculation has been presented by Harrison for Al,[4] achieving only a poor agreement with experiment. The calculations presented by Coulthard[15] and Williams and Appapillai,[16] based on the optimized Heine-Abarenkov-Shaw model potential (OMP)[17–21] are of intermediate nature, since only atomic data are used to fit the parameters of this potential. Coulthard[15] achieved nearly perfect agreement, using the full nonlocal form of the potential and the exchange and correlation corrections to the Hartree dielectric function proposed by Shaw and Pynn.[22] The dispersion relations obtained by Williams and Appapillai[16] with the same potential, but the exchange and correlation corrections of Toigo and Woodruff,[23] differ from experiment by up to 25%. This underlines the importance of exchange and correlation between the conduction electrons in lattice-dynamical calculations, especially for multivalent metals.

The main source of difficulties in the first-principles pseudopotential approach arises not from the formalism itself, but from the construction of a proper crystal potential. These are connected with the electronic exchange and correlation interactions. They are of outstanding importance at three different stages of the calculation: (i) in the calculation of the core states, (ii) in the conduction-band–core exchange interaction, and (iii) in the screening calculation. In a recently presented series of papers,[24,25] one of us (J.H.) studied the influence of different varieties of the $X\alpha$ exchange and correlation approximation[26–28] for the core-core and conduction-band–core interaction and of different conduction-electron exchange and correlation corrections to the dielectric function[22,29–31] on a pseudopotential calculation of a wide range of

static crystal properties of the simple metals from lithium to tin. It was shown that, with a suitable choice of the conduction-band–core exchange parameter, a satisfactory agreement with experiment can be obtained for atomic as well as electronic properties.

In this paper, the $X\alpha$ pseudopotential method is applied to the calculation of the lattice vibrations in aluminum. It is shown that with the pseudopotential defined in Ref. 24 a good, but not complete agreement with experiment is obtained for the dispersion curves along the principal symmetry directions. The remaining discrepancies are possibly to be attributed to the too long range of the $(\rho_{\text{core}})^{1/3}$ approximation for the valence-core exchange interaction. A simple way to correct this problem has been proposed by Lindgren[32] and introduced in pseudopotential theory by Moriarty.[33,34] In this work, the Lindgren approach to the conduction-band–core exchange potential will be tested as an alternative formulation.

In Sec. II, 25 different approximations for the exchange interactions and the results of the calculation of the energy–wave-number characteristics are presented. In the following sections, these characteristics are applied to the calculation of the lattice dynamics (Sec. III) and of properties of the static crystal lattice (binding energy, structural stability, zero-pressure density, and compressibility), Sec. IV. In Sec. V the corresponding form factors are tested against electronic (band structure and liquid resistivity) data. In Sec. VI we try to summarize the consequences of our calculations.

II. $X\alpha$ METHOD AND PSEUDOPOTENTIAL THEORY

The expectation value of the total energy of the electronic system may be expressed in the form

$$\langle E\rangle=\langle T\rangle+\langle U_{\text{ne}}\rangle+\langle U^{C}_{\text{ee}}\rangle+\langle U^{X}_{\text{ee}}\rangle\ , \tag{1}$$

where T is the kinetic energy and U_{ne} describes the interaction of the electrons with the nuclei, U^{C}_{ee} is the Coulomb, and U^{X}_{ee} is the exchange and correlation interaction between the electrons. At this point, the local statistical approximation is introduced: U^{X}_{ee} is approximated by a term proportional to the exchange energy per particle of a homogeneous electron gas of the same local density ρ. In rydberg units we have

$$U^{X}_{\text{ee}}=-9\alpha[3\rho(r)/8\pi]^{1/3}\ , \tag{2}$$

where α is a constant to be determined. An effective Schrödinger equation for the set of one-electron functions u_i may be deduced from the energy expression using the conventional variational ansatz. We obtain

$$(-\Delta+U_{\text{ne}}+U^{C}_{\text{ee}}+V^{X}_{\text{ee}})u_i=\epsilon_i u_i\ , \tag{3}$$

with the local statistical exchange potential $V^{X}_{\text{ee}}=\frac{2}{3}U^{X}_{\text{ee}}$. This variational argument has first been used by Kohn and Sham[35] with $\alpha=\frac{2}{3}$. Previously, Slater[36] proposed a factor of $\alpha=1$. A value between these extremes is better than either limiting value. For atomic calculations, different criteria[26,37–39] for the choice of the parameter α have been proposed. Of these, the method using the virial theorem, suggested by Berrondo and Goszinski[37] and Sham[38] and applied by Schwarz[27] to a large variety of atoms, allows the most accurate determination of the exchange parameter. With this optimized parameter α_{vt}, the $X\alpha$ energy agrees well with the Hartree-Fock (HF) energy, and the $X\alpha$ orbitals reproduce the HF orbitals fairly well. Moreover, it can be shown that the $X\alpha$ method is not merely an approximation to the HF theory, but is in some respects superior to it.[26,40,41] For the lightest atoms, the α_{vt} values are about 0.77, decreasing rapidly as the atomic number increases. The reasons for this variation have been investigated by Lindgren and Schwarz.[28] A single exchange parameter does not fit equally well all orbitals of an atom, the inner shells require a higher α than the outer ones, the self-interaction part requires a considerably larger α than the interelectronic part of the exchange interaction. It has been shown[24] that this last point is crucial for the correct description of the conduction-band–core exchange interaction.

There are two fundamental functions which enter in the general theory of pseudopotentials: (i) the pseudopotential form factor $\langle\vec{k}+\vec{q}\,|\,w\,|\,\vec{k}\rangle$ which describes the electronic properties of the metal, and (ii) the energy–wave-number characteristic determining the atomic properties. The form factor consists of the Fourier transform of a local crystal potential, a nonlocal repulsive term, and a screening potential arising from the conduction-electron interaction (for any details see Ref. 4 and our earlier work, Refs. 24, 25, 42–44). The crystal potential is builtup by the Coulomb potential of the atomic nuclei and the core electrons, the orthogonalization hole potential, and the exchange potential between the core and the valence electrons. The statistical approximation really applies to the *total* electronic charge density of the system. Because of the $(\rho_c+\rho_v)^{1/3}$ dependence of the total exchange potential, it is impossible to factor out the conduction-band–core part of the exchange interaction unequivocally. We therefore decided to use two different possible formulations: Formulation (i),

$$V^{X}_{K}(r)=-6\alpha_{1e}(3/8\pi)^{1/3}\rho_c(r)^{1/3}\ . \tag{4}$$

This is the form conventionally used in pseudopotential theory[4] and in our previous calculations.[24,25,42–44] It has the disadvantage of overes-

TABLE I. Short-hand notation for the bare pseudopotentials used in the calculations.

Pseudopotential	Valence-core exchange potential	α_c	α_{ie}
$K1$		0.72795[a]	0.3750
$K2$	$V_K^X = -6\alpha_{ie}[(3/8\pi)\rho_c]^{1/3}$	0.72795	0.4380[b]
$K3$		1.00000	2/3
$L1$	$V_L^X = -6\alpha_{ie}(3/8\pi)^{1/3}$	0.72795	1.3000
$L2$	$\{(\rho_c+\rho_v)^{1/3} - \rho_v^{1/3}\}$	1.00000	1.4000

[a] α_{vt}, optimized exchange parameter for the free atom (Ref. 27).

[b] Interelectronic exchange parameter describing the 3s-core interaction in the free atom (Ref. 28).

timating the range of the exchange interaction. Moreover, the interelectronic character of the valence-core exchange interaction has to be considered. This together yields optimal values of α_{ie} which are always notably smaller than the free-electron value $\alpha = \frac{2}{3}$. For Al, a value between $\alpha_{ie} = 0.375$ and 0.438 (this is the value determined by Lindgren and Schwarz[28] for the 3s-core interaction in the free atom) gives a very good description of the properties of the static lattice.[24,25] Therefore, these two values will be used here.

A second possibility is to isolate the self-exchange among the conduction electrons and to formulate the remaining part of the potential: Formulation (ii),

$$V_L^X(r) = -6\alpha_{ie}(3/8\pi)^{1/3}\{[\rho_c(r)+\rho_v(r)]^{1/3} - \rho_v(r)^{1/3}\} . \tag{5}$$

Since we have no *a priori* information about the charge density of the valence electrons in the metal, we approximate it by a homogenous distribution $\rho_v = Z/\Omega_0$, where Z is the valence and Ω_0 is the atomic volume. This is certainly consistent to zeroth order with our general approach. Outside the core, $\rho_v \gg \rho_c$, and the potential rapidly drops to zero. However, with this choice of ρ_v, ρ_v is not small enough compared to ρ_c inside the core, and the ansatz (ii) considerably reduces the magnitude of the exchange potential within the atomic sphere. It will turn out (cf. Sec. III) to be necessary to compensate for this fact by choosing a much greater α_{ie} than when using the form V_K^X.

The nonlocal repulsive contribution to the pseudopotential depends on the core wave functions as well as on the $q = 0$ component of the crystal potential. The core orbitals are calculated with the Herman-Skillman atomic structure program,[45] the local $X\alpha$ approximation with a variable exchange parameter α_c again being used for the description of the exchange interaction among the core electrons. To test the influence of this parameter upon the results of the calculations, we used the optimized value α_{vt} of Lindgren and Schwarz[28] (for Al, $\alpha_{vt} = 0.72795$) and the Slater value $\alpha_c = 1$ as well. Table I gives a short-hand notation for the bare pseudopotentials calculated with different forms of the valence-core exchange potential V^X and different exchange parameters α_c and α_{ie}.

The screening potential is calculated with the full nonlocal form of the pseudopotential (cf. Refs. 24, 25, and 43). In order to investigate the effect of exchange and correlation between the conduction electrons, we used several different forms of the dielectric function. In terms of the random-phase (or Hartree) dielectric function $\epsilon_H(q)$, $\epsilon(q)$ is given by

$$\epsilon(q) = 1 + [1 - f(q)]\epsilon_H(q) . \tag{6}$$

The function $f(q)$ appearing in (6) describes the corrections due to exchange and correlation. In the last years, a number of different approximate expressions for this function have been proposed.[22,29-31,46,47] Some examples being used in this work are listed in Table II.

The normalized energy-wave-number characteristics are calculated with the full nonlocal pseudopotentials. In Fig. 1 we plot the characteristics computed with the five pseudopotentials introduced above and with the Hubbard-Sham[46,47] (HS) screening function, appropriate to an atomic volume of $\Omega_0 = 111.4$ a.u. The general trends in the influence of the exchange parameters and of the screening function have been discussed in Ref. 24. However, it is important to emphasize that the choice of the Lindgren form for the conduction-band–core exchange results in a considerable reduction of the normalized characteristic in the range of intermediate and high wave number. The typical minimum in $F_N(q)$ is shifted towards greater values of the wave-number vector and the subsequent maximum is strongly reduced (in the case of pseudopotential $L1$, they are nearly completely smoothed out). We can therefore expect that the structural energy differences are severely reduced when this approach is used.

In the following sections, these characteristics will be applied to the calculation of dynamic and static crystal properties.

III. LATTICE DYNAMICS

A. Dispersion relations

The calculation of phonon dispersion relations within the framework of the pseudopotential theory is straightforward and is described, e.g., by Harrison[4] and by Heine and Weaire.[50] The results of our calculations, using the pseudopotentials $K1$ and $K2$, and the Kleinman-Langreth screening function are presented in Fig. 2. With potential $K1$, the longitudinal modes are nearly perfectly

TABLE II. Exchange and correlation corrections to the dielectric function.

	$f(q)$	$\lim f(q)\ k_F^2/q^2$ $q\to 0$	$\lim f(q)$ $q\to\infty$
Hartree approximation	0	0	0
Hubbard–Sham[a] (HS), Refs. 46, 47	$\frac{1}{2}\frac{q^2}{q^2+\gamma k_F^2}$	$\frac{1}{2\gamma}$	$\frac{1}{2}$
Singwi *et al.* (SSTL), Ref. 29	$A[1-\exp(-Bq^2/k_f^2)]$	AB	$A\sim 1$
Kleinman-Langreth[b] (KL), Refs. 30, 31	$\frac{1}{4}\left(\frac{q^2}{q^2+k_F^2+k_s^2}+\frac{q^2}{k_F^2+k_s^2}\right)$	$\frac{1}{2(1+k_s^2/k_F^2)}$	∞
Shaw-Pynn[c] (SP), Ref. 22	$\frac{1}{2}(1-\exp[-q^2/\beta\, k_F^2)]$ $+\frac{\gamma q^2}{k_F^3}\exp(-\alpha q^2/\gamma\, k_F^2)$	$1/2\beta+\gamma/k_F$	$\frac{1}{2}$
	$\beta=2,\ \gamma=0.0123,\ \alpha=0.0538$		

[a] γ may be calculated from $\gamma=2/[1+0.153/(\pi k_F)]$ (Ref. 48) such that $\epsilon(q)$ satisfies the compressibility sum rule with the Nozières-Pines interpolation formula (Ref. 49).

[b] In our calculation, we choose $k_s=(4k_F/\pi)^{1/2}$ to be the inverse Thomas-Fermi screening length. The compressibility sum rule is then only slightly violated.

[c] A value of $\beta=2$ corresponds to the Kohn-Sham approximation for exchange between the conduction electrons. The compressibility sum rule is satisfied by construction.

reproduced, but the transverse branches lie somewhat too high, especially in the [110] and [111] directions. With an enhanced conduction-band–core exchange potential ($K2$), the indirect ion-electron-ion interaction is reinforced, the negative band-structure contributions to the squared phonon frequencies are increased, and the dispersion curves lie deeper. As is to be expected, the longitudinal modes are somewhat more affected by the change in the exchange potential than the transverse branches. With a still greater exchange parameter (e.g., $\alpha_{ie}=\frac{2}{3}$), the phonon frequencies become imaginary over at least a part of the Brillouin zone. This is also valid when the core wave functions are calculated in the Slater approximation ($\alpha_c=1$). Only when the screening is treated in the Hartree approximation (cf. below), the phonon energies calculated with potential $K3$ (or with a potential corresponding to $\alpha_c=\alpha_{vt}$ and $\alpha_{ie}=\frac{2}{3}$) are real throughout, but are much too low.

To investigate the influence of the exchange and correlation corrections to the Hartree screening function, we replaced the Kleinman-Langreth[30,31] (KL) dielectric function in pseudopotential $K1$ by the other functions listed in Table II, and calculated the dispersion curves. The results are shown in

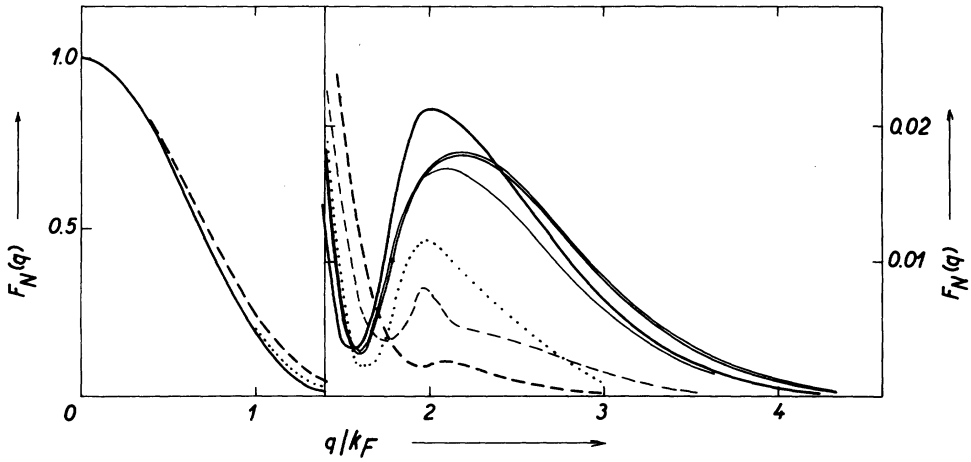

FIG. 1. Normalized-energy wave-number characteristics calculated with the KS approach (solid lines, bold: pseudopotential $K1$; thin line: $K2$, double line: $K3$), the L approach to the conduction-band–core exchange interaction (dashed lines, bold: $L1$; thin line: $L2$), and the HS screening function. The dotted curve represents the OMP characteristic (Ref. 16).

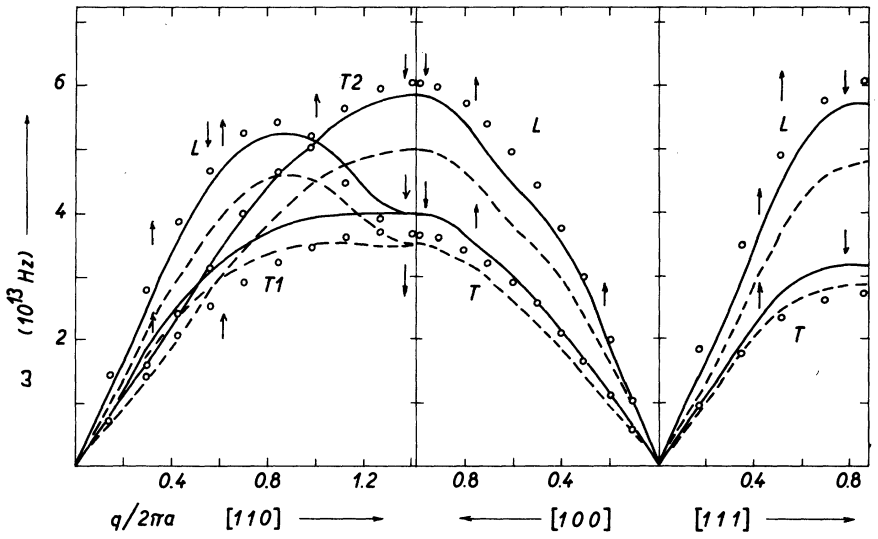

FIG. 2. Phonon dispersion relations in the principal symmetry directions, computed with the KS approach to the valence-core exchange and the KL screening function (solid line: pseudopotential $K1$, dashed line: $K2$). The experimental points are taken from Stedman and Nilsson (Ref. 51). The vertical arrows indicated the theoretical site and direction of the Kohn anomalies for a spherical Fermi surface.

Fig. 3. Generally, the influence of the screening function upon the longitudinal modes is much stronger than on the transverse ones. The frequencies calculated in the Hartree approximation for the screening are much too high, those computed with the HS function nearly coincide with the KL result. When the Shaw-Pynn[22] (SP) or Singwi-Sjölander-Tosi-Land[29] (SSTL) functions are used, the transverse frequencies are only slightly affected, but the longitudinal modes are sensibly reduced, especially in the SSTL approach. This shows that a correct relation between the longitudinal and the transverse branches is obtained only when the compressibility sum rule is at least approximately satisfied. When the parameter B in the SSTL function is adapted to satisfy the compressibility sum rule and A is chosen in order to yield a positive electron pair correlation function in the limit $r \to 0$, as proposed by Schmuck,[12] the longitudinal frequencies are increased and the agreement with experiment is greatly improved. On the other side, the limit of the exchange and correlation correction for very small wavelength is of minor importance in phonon calculations. This can be seen by comparing the results obtained in the HS and KL approximations [$\lim_{q\to\infty} f(q) = \frac{1}{2}$ in the HS approximation and ∞ in the KL approximation.] It is also interesting to collate the SP and HS results. By construction, both $f(q)$ functions satisfy the compressibility sum rule and have the same limiting value $f(q) \to \frac{1}{2}$ for large wave vectors. Nevertheless, the energy of the longitudinal pho-

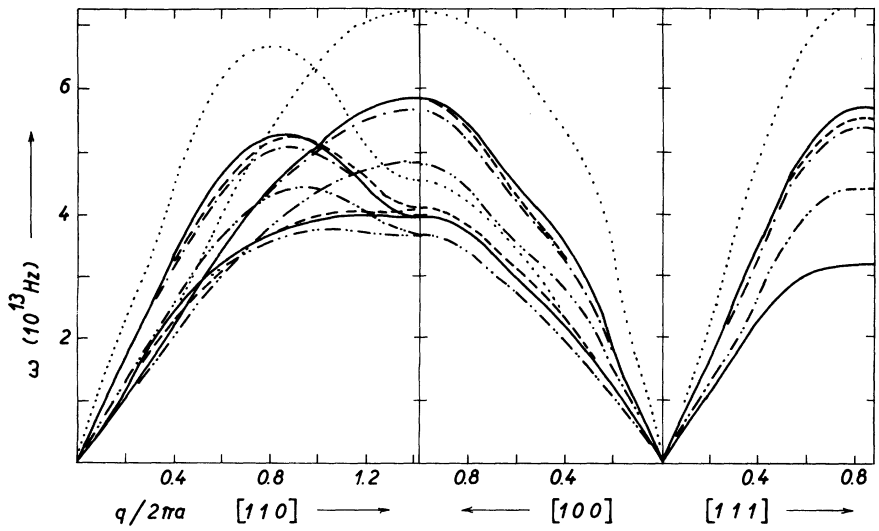

FIG. 3. Phonon dispersion relations calculated with pseudopotential $K1$ and different dielectric functions. Solid line: KL; dashed line: HS; dot-dashed line: SP; dash-dot-dot line: SSTL; dotted line: Hartree (see Table II).

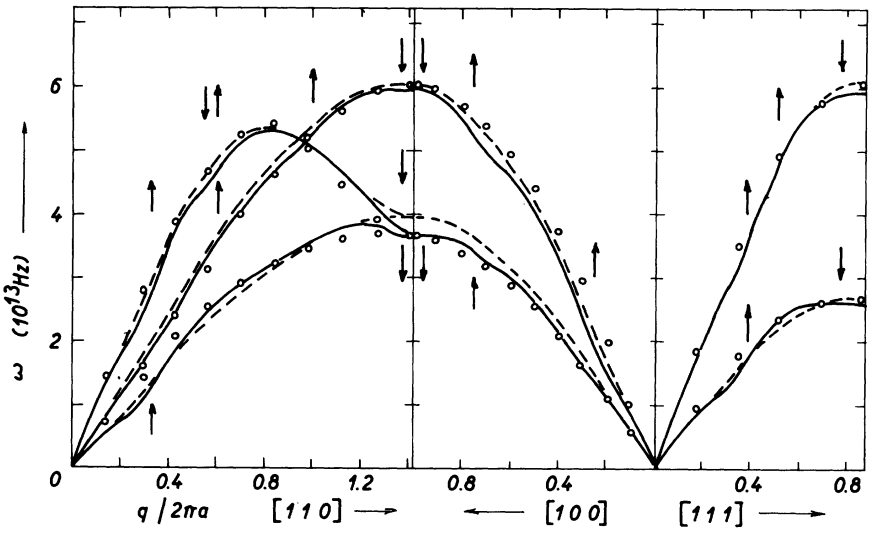

FIG. 4. Phonon dispersion relations computed with the L approach to the valence-core exchange interaction and the HS screening function (solid line: pseudopotential $L2$; dashed line: $L1$). The experimental points are taken from Stedman and Nilsson (Ref. 51). The vertical arrows indicate the theoretical site and direction of the Kohn anomalies.

nons is always smaller when calculated in the SP approximation. This can tentatively be attributed to the faster increase of the SP $f(q)$ for small and intermediate wave vectors: A greater $f(q)$ reduces the screening potential, therefore enhancing the negative band-structure contributions to the squared phonon frequencies. This would also explain the relatively poor results obtained with the SSTL function: Even when adjusted to fit the compressibility sum rule, $f_{\mathrm{SSTL}}(q)$ increases more rapidly than any other of the exchange correction functions. Although the KL function yielded the best result, a slight change in the screening constant k_s would alter the situation. A KL function with k_s adjusted to fit the compressibility sum rule increases steeper than the HS function and would therefore yield lower phonon energies. Within this approximation for the conduction-band–core exchange it appears to be impossible to close the remaining gap between theory and experiment by choosing another screening function.

Therefore we decided to use the Lindgren approach to the valence-core exchange [Eq. (5)]. With the same α_{le}, the spatial average of the exchange potential is then strongly reduced with respect to the Kohn-Sham approximation. Hence it is not surprising that the phonon energies calculated with V_L^X, $\alpha_c = \alpha_{\mathrm{vt}}$, and $\alpha_{\mathrm{le}} = 0.375$ or 0.438 are much too high. To obtain agreement with experiment, it turns out to be necessary to choose $\alpha_{\mathrm{le}} = 1.3$ (for $\alpha_c = \alpha_{\mathrm{vt}}$, potential $L1$), respectively, $\alpha_{\mathrm{le}} = 1.4$ (for $\alpha_c = 1$, $L2$). With these two possible

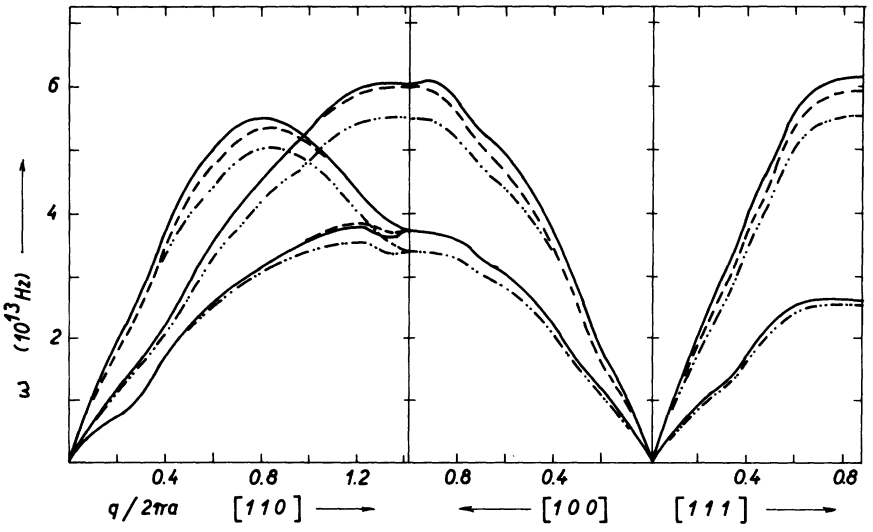

FIG. 5. Phonon dispersion relations computed with pseudopotential $L2$ and different screening functions. Solid line: KL; dashed line: HS; dot-dot-dash line: adjusted SSTL (see Table II and text).

choices of the exchange parameters and the HS dielectric function, the theoretical result nearly perfectly reproduces the measured phonon spectrum (Fig. 4). We are now to interpret the great values of the interelectronic exchange parameters. It is important to note that the spatial averages over the atomic sphere ($r_0 = 2.985$ a.u. for Al), $\langle V^X_{L1}\rangle_{av} = -0.1743$ Ry, $\langle V^X_{L2}\rangle_{av} = -0.1786$ Ry, $\langle V^X_{K1}\rangle_{av} = -0.141$ Ry, and $\langle V^X_{K2}\rangle_{av} = -0.1648$ Ry are approximately of the same magnitude. The main features of the phonon spectrum, namely, the frequencies at the zone boundary, are determined by the spatial average of the conduction-core exchange potential. The spatial variation of this potential is, however, important for the correct shape of the dispersion curves: e.g., the unrealistic crossing of the transverse branches in the [110] direction is removed when the unsatisfactory behavior at long distances of the $\rho_c^{1/3}$ approach is compensated by the choice of the Lindgren potential.

Here again we have tested the influence of different exchange and correlation corrections to the dielectric function (Fig. 5). The effect is much the same as described above, but a bit less pronounced. Again the results calculated with the HS and KL functions are almost identical, but also the modified SSTL function yields nearly as good a description of the dispersion curves.

B. Kohn anomalies

In our calculations we used a fine mesh of 40 equidistant points for the values of the wave vector in each symmetry direction. This was necessary to discern Kohn anomalies in the dispersion curves, where they appear as slightly s-shaped wiggles (see Figs. 2 and 4, the theoretical site and direction of the anomalies are indicated by the vertical arrows). They are only moderately expressed for the potentials $K1$ and $K2$, but appear very distinctly for potential $L2$, because of the sharp maximum in the characteristic. For $L1$, they are smoothed out because of the near coincidence of the minimum in $F_N(q)$ and the subsequent maximum at $q = 2k_F$. Examples for $\Delta\omega/\Delta q$ for q in the [100] direction are given in Fig. 6 for the pseudopotentials $K1$ and $L1$ and the HS screening. The Kohn anomalies are exhibited very accurately and can be seen very clearly, much more clearly than in the experimental curves with their finite resolution. The experimental points are those given by Stedman and Nilsson[51] and show that Kohn anomalies shifted due to the nonsphericity of the Fermi surface.

In summary, these results suggest that the accuracy of our characteristics is good and that the tabular interval of $0.05k_F$ chosen for the interpolation is small enough to allow even details of the function to be adequately reproduced. From all other phonon calculations presented for Al,[3-16] only those of Schmuck[12] and Williams *et al.*[16] show Kohn anomalies in the dispersion relations. In view of the investigations of Appapillai and Williams,[16] this casts some doubt on the numerical accuracy of the other calculations.

C. Effective interionic pair potential, elastic shear constants

It is interesting to throw a rapid look on the effective interionic pair potential V_{eff}, although we did not use it in our phonon calculations (which were performed in $\vec{k}$ space). V_{eff} is the sum of the direct Coulomb repulsion and an indirect ion-elec-

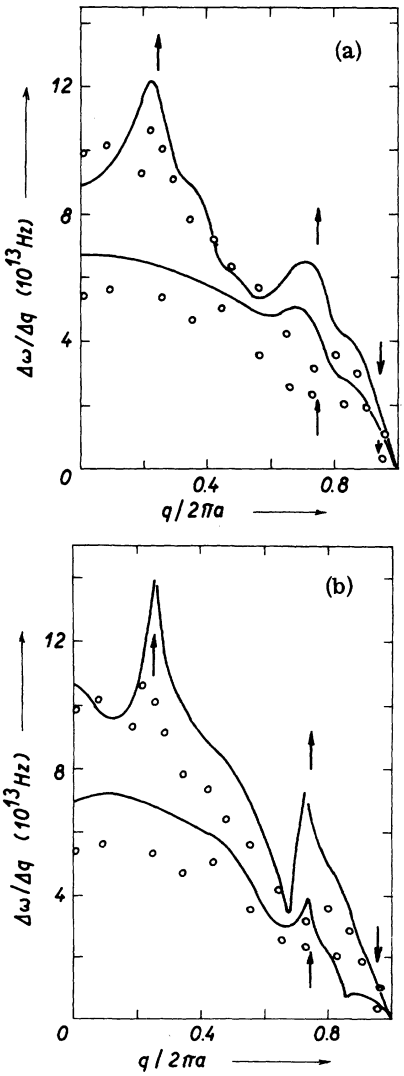

FIG. 6. $\Delta\omega/\Delta q$ in the [100] direction calculated with the HS screening function and pseudopotential, respectively, (a) $K1$ and (b) $L2$. The experimental points are those of Stedman and Nilsson (Ref. 51). The arrows indicate the theoretical site and direction of the Kohn anomalies for a spherical Fermi surface.

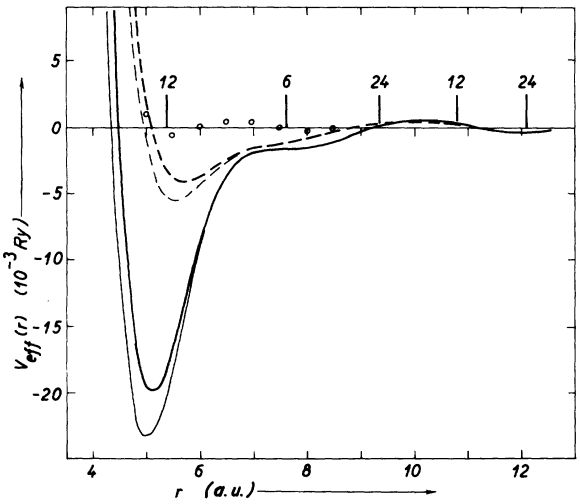

FIG. 7. Effective interionic pair potentials, calculated with different pseudopotentials. Same symbols as Fig. 1. The circles represent the pair potential of Shyu *et al.* (Ref. 51), computed with the OMP and SSTL screening. The vertical bars indicate the position of the next-nearest neighbors in the fcc lattice, the coordination number is given on the top of the bar.

tron-ion interaction represented by the Fourier transform of the normalized characteristic.[4,25] The prominent features of the metallic pair potentials are a deep minimum at the nearest-neighbor distance and the long-range Friedel oscillations.[4] The influence of the core-core, the valence-core (with the $\rho^{1/3}$ approach), and the valence-valence exchange interactions has recently been discussed by Hafner.[25] Thus we may confine ourselves, here, to present the pair-potentials computed with the pseudopotentials $K1$ to $L2$ and the HS screening function (Fig. 7). It is shown that the main characteristics are unchanged when the V_K^X conduction-core potential is replaced by the V_L^X approximation, but the first minimum is slightly shifted towards greater distances, and it's depth is strongly reduced. This brings the potential into closer agreement with the OMP result of Shyu *et al.*[52] [Shyu *et al.* used the SSTL dielectric function; when we replace the HS function in our potential $L1$ by the SSTL form, this results in a still shallower minimum (2.5×10^{-3} Ry for SSTL, 4.05×10^{-3} Ry for HS at $r=5.6$ a.u.).] Recalling that in a first approximation the phonon frequencies depend on the shape of the effective interionic potential at the nearest-neighbor shells, we expect V_{eff} calculated in the V_L^X approximation to be the more realistic one. This may be checked by computing the elastic shear constants using the method proposed by Squires.[53] The results are entirely consistent with our phonon calculations: In the V_K^X approach, $C'=\frac{1}{2}(C_{11}-C_{12})$ turns out to be greater than C_{44}—this corresponds to the crossing of the transverse branches in the [110] direction. With the V_L^X exchange potential and the HS dielectric function we obtain (in units of 10^{11} dyn/cm^2) $C_{44}=4.28$ ($L1$), $C_{44}=3.15$ ($L2$), $C'=2.52$ ($L1$), and $C'=3.04$ ($L2$). However, due to the well-known convergence difficulties associated with this method,[11] the accuracy of these results is certainly not better than 10%. With this restriction, the agreement with the experimental values of Kamm and Alers[54] ($C_{44}=3.16$, $C'=2.62$) is rather good.

IV. CRYSTAL BINDING

A. Structural energies

We have used the conventional second-order perturbation theory[4,50] for the calculation of the structure-dependent parts of the binding energy for the face-centered tetragonal structures as a function of the axial ratio ($c/a=1$ corresponds to face-centered cubic, $c/a=1/\sqrt{2}$ to body-centered cubic), for the hexagonal close-packed lattice as a function of c/a, for rhombohedrally distorted fcc structures (a compression of $\delta=1.585$ along the axis of distortion corresponds to the simple cubic (sc) structure) and in the orthorhombic GaI lattice. In Table III we have listed the computed energy differences relative to the energetically most favorable structure, calculated with the pseudopotentials $K1$ to $L2$ and different screening functions, together with the corresponding OMP results of Williams and Appapillai[16] and some available thermochemical estimates for these quantities. Except for potential $K3$ (which has already been recognized to be unrealistic), fcc is the stable phase in each case. The structure is also seen to be stable against both tetragonal and rhomboedral shear.

The energy differences are only slightly affected by the choice of the screening function. As is to be expected from the form of the normalized characteristics, these differences are strongly reduced when the Kohn-Sham form for the conduction-core exchange potential is replaced by the Lindgren approximation. The thermochemical estimates for the structural energy differences given by Kaufman and Bernstein[55] and Lupis[56] may be used as reference values. However, the large differences in the estimates for the energy difference between the fcc and hcp phases shows that they must be regarded with some reserve. In each case it seems to be reasonable to assume that ΔE should not be, at least for close-packed structures, greater than the heat of fusion (for Al, $\Delta E_{\text{solid liquid}}=81.9\times10^{-4}$ Ry[57]). Hence it appears that the pseudopotentials $K1$ and $K2$ overestimate the structural energy differences, whereas those computed in the Lindgren approximation are rather too small (especially for

TABLE III. Calculated energy differences relative to the energetically most favorable structure and equilibrium axial ratio in the hexagonal phase.

Pseudo-potential	Screening function	ΔE (10^{-4} Ryd) fcc	bcc	hcp	c/a	sc	GaI
$K3$	SSTL	82.4	185.2	111.3	Ref. a	44.5	0
$K2$	SSTL	0	106.7	18.7	1.72	203.0	54.4
$K1$	SSTL	0	130.4	35.1	1.70	384.0	98.0
$L1$	SSTL	0	36.2	0.7	1.73	176.6	236.2
	HS	0	33.0	1.0	1.69	285.9	353.0
$L2$	SSTL	0	56.1	7.1	1.75	203.5	223.5
	HS	0	51.2	8.1	1.71	282.9	335.5
OMP (Ref. 16)		0	106.4	29.2	1.73	175.1	140.6
thermochemical estimates	Ref. 55	0	77.0	41.8			
	Ref. 56	0		3.8			

[a]The hexagonal structure is instable against shear deformation in the calculated range of the axial ratio ($c/a = 1.5$–2.0). The energy difference is quoted against the ideal hcp structure.

the hcp structure, see below).

The absolute values for the calculated binding energy at the observed density are (in Ry) $E_B = -4.185$ ($K1$), -4.245 ($K2$), -4.266 ($L1$ SSTL), -4.260 ($L1$ HS), -4.211 ($L2$ SSTL), and -4.208 ($L2$ HS). For the potentials $K1$ and $L2$ they compare favorably with the experimental value $E_B = -4.171$ Ry.

B. Equilibrium lattice spacing and binding energy

For a complete description of the cohesive properties it is necessary that the calculation yields not only a correct binding energy at the observed density, but also a reasonably accurate zero-pressure density. For this purpose, we varied the atomic radius and computed the equilibrium lattice spacing, the corresponding binding energy and compressibility with the methods outlined in our previous work.[24] The results are compiled in Table IV. The atomic radii calculated with the Kohn-Sham approach agree with experiment within 3%, whereas those calculated using the Lindgren approximation differ by as much as 10% from the measured value, and the accuracy of the computed binding energies is also reduced. The differences between the Kohn-Sham (KS) and the L approach stem from a different variation of the band-structure energy E_{bs} with the atomic volume: For the pseudopotentials $K1$ to $K3$, E_{bs} is nearly constant over the whole range of the atomic radius considered in these calculations ($\pm 10\%$ of the observed radius). In opposition thereto, E_{bs} is more than doubled for the potentials $L1$ and $L2$, when the atomic radius is increased from 0.90 to 1.15 of its observed value. This different behavior can be explained by considering the different shape of the normalized characteristics (cf. Fig. 1). For the potentials $K1$ and $K2$ (and, as should be noted, for the OMP potential), the first minimum lies between the two shortest vectors of the wave-number lattice of the fcc structure ($q_1/k_F = 1.54$, $q_2/k_F = 1.77$), whereas for $L1$ and $L2$ it lies beyond q_2. For the expanded lattice, the site of the minimum in F_N travels towards a greater q/k_F. Therefore, the contribution of q_1 to E_{bs} is increased, whereas that of q_2 decreases for the potentials $K1$ and $K2$, thus E_{bs} remains essentially constant. On the other side, both contributions increase for the potentials $L1$ and $L2$. This behavior is contrary to what is generally expected in pseudopotential theory. In spite of the excellent results obtained for the lattice dynamics, this casts some doubt on the appropriateness of the Lindgren approximation in the case of Al. We shall explore this point further when considering the electronic properties.

In the two last columns of Table IV we listed the isothermal compressibility K_T and the ratio between K_T and the compressibility of a noninteracting electron gas of the same density, K_0. It can be seen that the theory considerably underestimates the compressibility of the metal. The reason for that is not completely clear, but lies perhaps in the assumption of a rigid core over a very wide compression range.

The large difference between the equilibrium value of the atomic radius and its experimental size in the Lindgren approximation rises still another difficulty: we cannot assume the very small structural energy differences to be independent of the atomic volume. Hence we computed the structural energy differences between the common metallic structures (fcc, bcc, hcp) as a function of the

TABLE IV. Equilibrium atomic radius, binding energy, and isothermal compressibility.

Pseudopotential	Screening function	r_0 (a.u.)	E_B (Ry)	K_T[(a.u.)^3/Ry]	K_T/K_0[a]
$K3$	SSTL	2.91	−4.453	101	2.21
$K2$	SSTL	3.05	−4.248	148	2.56
$K1$	SSTL	3.07	−4.189	137	2.33
L_1	SSTL	3.28	−4.299	216	2.59
	HS	3.25	−4.288	193	2.43
$L2$	SSTL	3.29	−4.243	238	2.82
	HS	3.26	−4.235	211	2.51
experiment		2.98	−4.171	185.5[b]	3.6

[a]K_0 is the compressibility of a noninteracting electron gas of the same density.
[b]Reference 54.

atomic radius. The results are given in Table V. The energy differences are seen to vary continuously with the atomic radius, those between the cubic lattices increase with increasing compression. The energy difference between the fcc and the hcp phases decreases when the crystal is expanded. Moreover, there is a progressing tendency for the hcp structure to distort; whereas an augmented density favors a structure which is nearer to the ideal close packing. Unfortunately it must be recognized that the most stable structure at the theoretical zero-pressure density is a distorted hcp phase, when we use the Lindgren approximation for the valence-core exchange. On the other hand, nothing is changed against the calculations at the observed density with the KS approach, the energy differences are only slightly reduced, improving the agreement with experiment.

Hence we are led to conclude that, in spite of the excellent results obtained for the phonon energies, the Lindgren approximation does not lead to a satisfactory description of the structural and cohesive properties of aluminum.

V. ELECTRONIC PROPERTIES

We are now to test our pseudopotentials against electronic properties. Instead of performing a complete band-structure calculation, we restricted ourselves to compare our OPW form factors (with the conventional on Fermi-sphere geometry) with the empirical form factors fitted to the Fermi surface,[58] optical data,[59] and to the soft x-ray spectrum[60] (Fig. 8). It can be seen that the $K1$ and $K2$ form factors pass slightly above the empirical points, whereas the $L1$ and $L2$ curves are definitely too low. This is independent from the choice of the

TABLE V. Variation of the structural energy differences relative to the face-centered cubic phase, ΔE(fcc-bcc, hcp) with the atomic radius.

	Pseudopotential	Screening function	ΔE (10^{-4} Ry)				
	r_0/r_0 (expt)		0.90	0.95	1	1.05	1.10
bcc	$K1$	SSTL		159.1	130.4	101.5	76.0
	$K2$	SSTL		145.4	106.7	99.4	65.3
	$L1$	SSTL	57.4	46.6	36.2	25.3	15.8
	$L1$	HS	52.8	42.8	33.0	23.3	14.8
	$L2$	SSTL	90.6	73.8	56.1	39.4	25.7
	$L2$	HS	83.5	68.4	51.2	35.8	23.5
hcp[a]	$K1$	SSTL		49.7(1.68)	35.1(1.70)	22.1(1.77)	8.1(1.80)
	$K2$	SSTL		42.8(1.69)	18.7(1.72)	14.6(1.80)	1.7(1.8)
	$L1$	SSTL	8.9(1.67)	4.4(1.69)	0.7(1.73)	−7.1(1.81)	−5.3(Ref. b)
	$L1$	HS	8.5(1.66)	4.5(1.68)	1.0(1.69)	−3.1(1.73)	−2.6(1.67)
	$L2$	SSTL	20.8(1.67)	15.4(1.70)	7.1(1.75)	−4.7(1.88)	−8.1(Ref. b)
	$L2$	HS	20.4(1.67)	14.5(1.69)	8.1(1.71)	0.3(1.75)	−5.9(1.82)

[a]The equilibrium axes ratio is given in parentheses.
[b]The hcp lattice is instable against shear deformation in the considered range of the axies ratio (c/a = 1.5–2.0). The energy differences refer to a structure with c/a = 2.0.

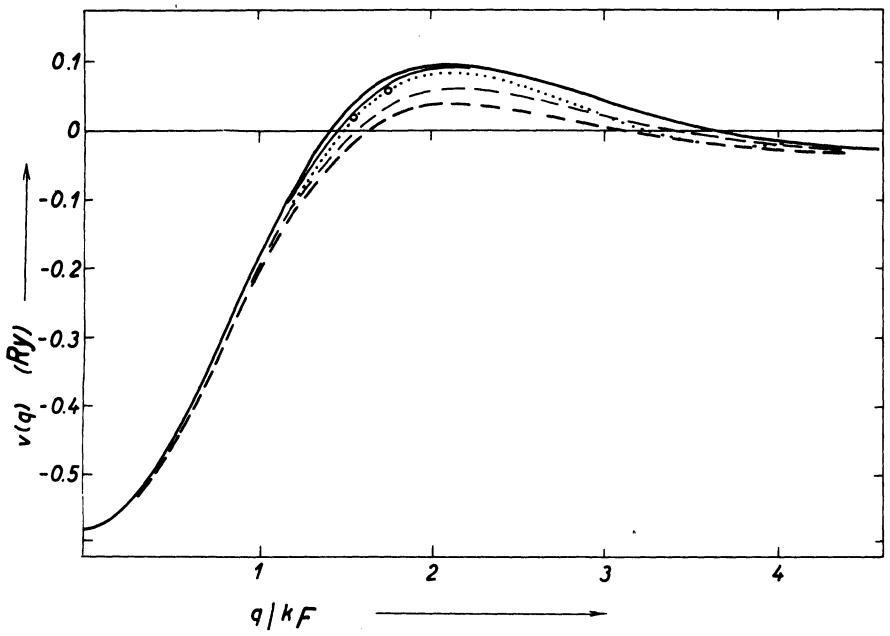

FIG. 8. OPW form factors for the different pseudopotentials. Same symbols as Fig. 1. The circles represent the empirical form factors (for references see text).

dielectric function. The OMP passes nearly exactly through the fitted points.

Another simple possibility to test the electronic scattering properties of the pseudopotential is to calculate the electrical resistivity of the liquid metal. Using the Ziman formula[61] with the Percus-Yevick hard-core structure factor,[62] a packing fraction of $\eta = 0.46$, and an atomic volume of $\Omega_0 = 128.96$ a.u. (this corresponds to the density of liquid Al at 785 °C), we obtained the results listed in Table VI. The structure factor for this temperature has recently been measured by inelastic neutron scattering and it has been shown that a hard-core model with $\eta = 0.46$ gives an excellent fit to the experimental values.[63] It should be pointed out that in our calculations, the form factor has been computed anew for the density appropriate to the melt, therefore the results do not involve any of the scaling assumptions for the pseudopotential as a function of the atomic volume usually made in such calculations. The peak of the structure factor (hard-core model and experimental) occurs at $q/k_F = 1.59$, this is within 0.03 of the first node of the form factors in the case of the $L1$ and $L2$ pseudopotentials. This leads to a very low value of the electrical resistivity. On the other side, the resistivities calculated within the KS approach and different screening functions are in good agreement; those computed with $K2$ are in even excellent agreement with experiment.[64] This is just what we expected from our comparison of the theoretical form factors with the empirical ones. Thus it appears that the Lindgren approximation is definitely inappropriate to a treatment of the electronic properties of metallic Al.

VI. CONCLUSIONS

The above results, while not being in perfect agreement with experiment for a single pseudopotential, are very instructive regarding the nature of the conduction-band–core exchange potential: For those properties depending only on the values of the characteristic of the form factor for wave numbers greater than the shortest vector in the wave-number lattice [structural and cohesive properties; electronic properties—although the electrical resistivity formally depends on an integral over q from 0 to $2k_F$, the particular form of the integrand heavily outweights the values of $v(q)$ at the upper boundary], the KS-approach of the $\rho_c^{1/3}$ type is more appropriate. On the other hand, the

TABLE VI. Electrical resistivity of liquid Al at 785 °K (in $\mu\Omega$ cm).

	Pseudopotential	Screening function	KL	SSTL	HS
Theory	$K1$		29.5	31.0	
	$K2$		24.9	26.3	
	$K3$		23.3	24.8	
	$L1$			15.5	13.0
	$L2$		13.7	15.1	13.3
Experiment (Ref. 64)				26.0	

L-approximation $(\rho_c+\rho_v)^{1/3}-\rho_v^{1/3}$ yields better results for properties depending also on the long-wavelength limit of the pseudopotential (phonon dispersion, interionic potential, and elastic shear-constants).

This can easily be understood: the $\rho_c^{1/3}$ approach is certainly a good approximation inside the ionic core (small r), but overestimates the range of the exchange potential. This is compensated in the $(\rho_c+\rho_v)^{1/3}-\rho_v^{1/3}$ approach, which in turn is certainly inappropriate inside the core. Fourier transforming the exchange potential, we expect the L-type potential to be more reliable for small q, while the KS approach should be more appropriate for larger wave numbers. Our results confirm these expectations: the pseudopotential $K2$, yielding the best results for cohesive and electronic properties, also gives the best description of the transverse phonon branches in the KS approach, while for the longitudinal modes, a slight modification of the potential ($K1$) is necessary to obtain agreement with experiment. For small q, this modification goes into the direction of the L-type pseudopotentials. These potentials ($L1$ and $L2$) produce phonon dispersion curves in nearly perfect agreement with experiment. However, we must reject them because they are not consistent with the structural, cohesive, and electronic band-structure data. It is of interest to mention that the form factor of these potentials closely resembles the local four-parameter model fitted to the phonon spectrum by Schneider and Stoll[5] and that it produces the same characteristic deviation from experiment in the low-q region of the [110] transverse branches. We refer to the comments of Cohen and Heine (Ref. 50, p. 109) regarding this potential. On the other hand, the OMP form factor and characteristic of Appapillai and Williams[16] are similar to our potentials $K1$ and $K2$ (see Figs. 1 and 7) and their phonon curves show the same unphysical crossing of the [110] transverse modes. Coulthards calculation[15] with the same potential, but a different screening function does not produce this particular feature. Why this is so remains an open question. From our results it appears unlikely that the different exchange and correlation corrections are responsible for this discrepancy.

Generally, we find a decrease in all phonon frequencies when going from the Hartree approximation to any other dielectric function containing exchange and correlation corrections, but the shape of the dispersion curves is essentially unchanged. The amount of the reduction depends primarly upon the low-q limit of the correction function $\lim_{q\to 0} f(q) \times k_F^2/q^2$: For those $f(q)$ yielding smaller values than required by the compressibility sum rule (KL), the frequencies are higher than for those satisfying this rule (SP, HS) or showing a deviation in the opposite direction (SSTL); and on the increase of $f(q)$ for small wave numbers. These results are in basic agreement with the findings of Coulthard[15] and Price *et al.*[65] They explain why the Toigo-Woodruff correction function[23] [which nearly satisfies the compressibility sum rule, but increases quadratically with q for small wave numbers—i.e., faster than any of the $f(q)$ functions tested in this work] employed by Williams and Appapillai[16] is inappropriate for phonon calculations. There is a strong evidence from these works[15,16] and ours that a screening function of the Hubbard-Sham or Shaw-Pynn type, adjusted to satisfy the compressibility sum rule is most suitable for phonon calculations in Al.

The exchange parameter α_c is only of minor importance: a different α_c may be largely compensated by a modified α_{1e}, so it becomes difficult to assess whether a variation of the results with α_c reflects a physical property of the system or simply a compensation of another shortcoming of the theory. In each case, the choice $\alpha_c=\alpha_{vt}$ is certainly well founded.

At first sight, our results appear to contradict the calculations of King and Cutler[66] on Be and Mg, using the same type of first-principles pseudopotential approach. They obtain excellent results for Mg, using $\alpha_c=1$, $\alpha_{1e}=\frac{2}{3}$, and a HS-type screening function, and they note a not perceptible influence of the exchange and correlation corrections to the dielectric function on the phonon energies in most branches. This is due to two important differences: (i) Their orthogonalization contribution to the core-energy shift is not consistent with Harrison's formulation (Ref. 4, p. 287: it should be noted that the formula given by Harrison is incorrect for a factor, $\frac{1}{2}$, but he quoted the correct numerical value). The difference acts in the same manner than Harrison's phenomenological correction to his Al pseudopotential (Ref. 4, p. 295), i.e., enhancing the phonon frequencies. It has been noted that such a correction goes in the opposite direction to that required to obtain a good description of the electronic properties. (ii) In the screening contribution to the characteristic, a factor $[1-f(q)]^{-1}$ is missing in their formulation. This explains the relatively small influence of the valence-valence exchange upon their results.

In summary, the application of the $X\alpha$ pseudopotential method to the theory of aluminum is quite hopeful, though a more refined treatment of the conduction-band–core exchange being valid both inside and outside the core appears to be desirable.

ACKNOWLEDGMENTS

One of the authors (J.H.) acknowledges useful correspondence with Professor P. H. Cutler and Dr. W. F. King. The numerical calculations were

performed using the computing facilities of the Interfakultäres Rechenzentrum der Universität Wien (IBM 360/44). The second author (P.S.) would like to express his thanks to Dr. M. Graef, Director of the Zentrum für Datenverarbeitung at the University of Tübingen, and to Professor Dr. K. Wirtz, Director of the Institut für Neutronenphysik und Reaktortechnik at the Nuclear Research Center, Karlsruhe, for providing the possibilities to perform part of this work at their institutes.

---

*Supported by the Fonds zur Förderung der wissenschaftlichen Forschung in Österreich under Project No. 1318.

†Part of the work described in this paper was performed while employed at the Computer Center of the University of Tübingen.

[1]T. Toya, J. Res. Inst. Catal., Hokkaido Univ. 6, 161 (1958).
[2]W. Cochran, Proc. Roy. Soc. Lond. A 276, 308 (1963).
[3]W. A. Harrison, Phys. Rev. 139, A179 (1965).
[4]W. A. Harrison, *Pseudopotentials in the Theory of Metals* (Benjamin, New York, 1966); Phys. Rev. 136, A1107 (1964).
[5]T. Schneider and E. Stoll, Phys. Kondens. Mater. 5, 331 (1966).
[6]T. Schneider and E. Stoll, *Neutron Inelastic Scattering* (IAEA Vienna, 1968), Vol. 1, p. 101.
[7]G. L. Krasko and Z. A. Gurskii, Fiz. Tverd. Tela 13, 2463 (1971) [Sov. Phys.-Solid State 13, 2062 (1972)].
[8]D. C. Wallace, Phys. Rev. B 1, 3963, 4521 (1970).
[9]H. C. Gupta and B. B. Tripathi, Phys. Rev. B 2, 248 (1970).
[10]D. C. Wallace, Phys. Rev. 187, 991 (1969).
[11]W. M. Hartmann and T. O. Milbrodt, Phys. Rev. B 3, 4133 (1971).
[12]P. Schmuck, Z. Phys. 248, 111 (1971).
[13]B. Prasad and R. S. Srivastava, Phys. Lett. A 38, 527 (1972).
[14]C. M. Kachlava, Physica 65, 63 (1973).
[15]M. A. Coulthard, J. Phys. C 3, 820 (1970).
[16]M. A ppapillai and A. R. Williams, J. Phys. F 3, 759 (1973); A. R. Williams and M. Appapillai, J. Phys. F 3, 772 (1973).
[17]V. Heine and I. V. Abarenkov, Phil. Mag 9, 451 (1964).
[18]A. O. E. Animalu, Phil. Mag. 11, 379 (1965).
[19]I. V. Abarenkov and V. Heine, Phil. Mag. 12, 529 (1965).
[20]R. W. Shaw, Jr. and W. A. Harrison, Phys. Rev. 163, 604 (1967).
[21]R. W. Shaw, Jr., Phys. Rev. 174, 769 (1968).
[22]R. W. Shaw, Jr. and R. Pynn, J. Phys. C 2, 2071 (1969).
[23]F. Toigo and T. O. Woodruff, Phys. Rev. B 2, 3958 (1971).
[24]J. Hafner, Phys. Status Solidi (B) 56, 579 (1973); 57, 101 (1973); 57, 479 (1973).
[25]J. Hafner, Acta Phys. Austriaca 38, 70 (1973).
[26]J. C. Slater and K. H. Johnson, Phys. Rev. B 5, 844 (1972).
[27]K. Schwarz, Phys. Rev. B 5, 2466 (1972).
[28]I. Lindgren and K. Schwarz, Phys. Rev. A 5, 542 (1972).
[29]K. S. Singwi, A. Sjölander, M. P. Tosi and R. H. Land, Phys. Rev. B 1, 1044 (1970).
[30]L. Kleinman, Phys. Rev. 160, 585 (1967).
[31]D. C. Langreth, Phys. Rev. 181, 753 (1969).
[32]I. Lindgren, Int. J. Quantum Chem. Symp. 5, 411 (1971).
[33]J. A. Moriarty, Phys. Rev. B 6, 1239 (1972).
[34]J. A. Moriarty, Phys. Rev. B 6, 4445 (1972).
[35]W. Kohn and L. J. Sham, Phys. Rev. 140, A1133 (1965).
[36]J. C. Slater, Phys. Rev. 81, 385 (1951).
[37]M. Berrondo and O. Goszinski, Phys. Rev. 184, 10 (1969).
[38]L. J. Sham, Phys. Rev. A 1, 969 (1970).
[39]I. Lindgren, Phys. Lett. 19, 382 (1965).
[40]A. W. Overhauser, Phys. Rev. B 3, 1888 (1971).
[41]K. J. Duff and A. W. Overhauser, Phys. Rev. B 5, 2799 (1972).
[42]J. Hafner and H. Nowotny, Phys. Lett. A 37, 395 (1971).
[43]J. Hafner and H. Nowotny, Phys. Status Solidi B 51, 107 (1972); Phys. Status Solidi B 55, 843(E) (1972).
[44]J. Hafner, Nuovo Cimento Lett. 5, 503 (1972).
[45]F. Herman and S. Skillman, *Atomic Structure Calculations* (Prentice, Englewood Cliffs, N. J., 1963).
[46]J. Hubbard, Proc. Roy. Soc. (Lond.) A 240, 539 (1957); A243, 356 (1957).
[47]L. J. Sham, Proc. Roy. Soc. (London) A283, 33 (1965).
[48]N. W. Ashcroft, J. Phys. C 1, 232 (1968).
[49]P. Nozières and D. Pines, Phys. Rev. 111, 442 (1958).
[50]V. Heine and D. Weaire, in *Solid State Physics*, edited by F. Seitz, D. Turnbull, and H. Ehrenreich (Academic, New York, 1970), Vol. 24, p. 242; M. H. Cohen and V. Heine, *ibid.*, p. 50.
[51]R. Stedman and G. Nilsson, Phys. Rev. 145, 492 (1966); Phys. Rev. Lett. 15, 634 (1965).
[52]W. M. Shyu, J. H. Wehling, M. R. Cordes and G. D. Gaspari, Phys. Rev. B4, 1802 (1971).
[53]G. L. Squires, Ark. Fys. 25, 21 (1963).
[54]G. N. Kamm and G. A. Alers, J. Appl. Phys. 35, 327 (1964).
[55]L. Kaufman and H. Bernstein, *Computer Calculations of Phase Diagrams* (Academic, New York, 1970).
[56]C. H. P. Lupis [unpublished result quoted by L. Kaufman, in *Metallurgical Chemistry Symposium*, 1971, edited by O. Kubaschewski (HMSO, London, 1972)].
[57]K. A. Gschneider, in Ref. 50, Vol. 16, p. 332.
[58]N. W. Ashcroft, Philos. Mag. 8, 2055 (1963).
[59]A. J. Hughes, D. Jones, and A. M. Lettington, J. Phys. C 2, 101 (1969).
[60]G. A. Rooke, J. Phys. C 1, 776 (1968).
[61]J. Ziman, Philos. Mag. 6, 1013 (1961).
[62]N. W. Ashcroft and J. Lekner, Phys. Rev. 145, 83 (1966).
[63]K. Kunsch, thesis (Technical University, Vienna, 1969) (unpublished).
[64]A. Roll and H. Motz, Z. Metallkd. 48, 272 (1957).
[65]D. L. Price, K. S. Singwi and M. P. Tosi, Phys. Rev. B 2, 2398 (1970).
[66]W. F. King and P. H. Cutler, Phys. Rev. B 2, 1733 (1970); Phys. Rev. B 3, 2485 (1971).